Results in Physics 35 (2022) 105392

Contents lists available at ScienceDirect

Results in Physics

journal homepage: www.elsevier.com/locate/rinp

Mathematical analysis of a COVID-19 model with double dose vaccination in Bangladesh

Anip Kumar Paul [a,b], Md Abdul Kuddus [a,*]

[a] Department of Mathematics, University of Rajshahi, Rajshahi 6205, Bangladesh
[b] Department of General Educational Development, Daffodil International University, Ashulia, Bangladesh

ARTICLE INFO

Keywords:
COVID-19 model
Vaccination
Stability and Sensitivity analysis
Bangladesh

ABSTRACT

COVID-19 is an infectious disease that kills millions of people each year and it is a major public health problem around the globe. The current COVID-19 situation is still now concerning, though the vaccination program is running. In this study, we considered a COVID-19 model with a double-dose vaccination strategy to control the current outbreak situation in Bangladesh. The fundamental qualitative analysis of this mathematical model has been performed. The conditions of positive invariance, boundedness with suitable initial conditions were analyzed. We have estimated the basic reproduction number ($\Re_0$) for disease transmission and determined that our model contains two equilibrium points: the disease-free equilibrium and a disease-endemic equilibrium. We used the Routh-Hurwitz criteria to determine the stability of the equilibria. The disease will be eradicated from the community if $\Re_0 < 1$, otherwise the disease persists in the population. To support the qualitative analysis of our model, we performed numerical simulations using MATLAB routine and estimated model parameters. Sensitivity analysis is used to explore the association for Mild and Critical cases concerning the corresponding model parameters. We observed that the most significant parameter to spread the virus is the transmission rate. The numerical simulations showed that a full dose vaccination program significantly reduces the mild and critical cases and has potential impact to eradicate the virus from the community. The information that we generated from our analysis may help the public health professionals to impose the best strategy effectively to control the outbreak situation of the virus in Bangladesh.

Introduction

Human being around the globe is now continuously facing major public health problem due to the spread of the SARS-CoV-2 virus. According to the mutation rate and severity of the virus, different variants of the SARS-CoV-2 have been identified [1]. The World Health Organization (WHO) estimated that there were approximately 248,467,363 infected cases, and 5,027,183 persons died due to COVID-19 whereas, 7,027,377,238 doses of vaccine have been administered up to November 4, 2021 [2]. Already, most of the countries in the world continued the second dose vaccination against the SARS-CoV-2 virus and considering buster dose vaccine for the near future. Therefore, the studies about the new infection and transmission of the virus after vaccination is a key concern. Mathematical models play an important role to explore the transmission dynamics of diseases and policy-makers can effortlessly evaluate the further health risk.

Since the middle of the 20th century, the transmission dynamic of infectious diseases outbreak can be analyzed with the help of deterministic and stochastic epidemiology models. Those models represent real-world phenomena and predict the severity of the infectious disease using mathematical concepts [3]. This research is motivated by the ongoing vaccination to protect the transmission of the novel coronavirus among human beings. Here, we developed a COVID-19 mathematical model to simulate the transmission and progression of the virus after one or second dose vaccination.

Transmission dynamics of any epidemiological infectious diseases are universal. Several researchers have been analyzed the transmission dynamics of coronavirus and presented different models. They studied and extended Susceptible–Exposed–Infected–Removed (SEIR) mathematical model with significant compartments to track and express the real phenomena. Muller and Muller, 2021 [4] presented a modified SEIR model to determine the transmission dynamics of the coronavirus on a college campus. They suggested as contact tracing can be an effective strategy to prevent the disease. The awareness programs and proper

* Corresponding author.
E-mail address: makuddus.math@ru.ac.bd (M.A. Kuddus).

https://doi.org/10.1016/j.rinp.2022.105392
Received 20 January 2022; Received in revised form 28 February 2022; Accepted 1 March 2022
Available online 2 March 2022

treatment, in hospital or isolation, of infected individuals, are the main steps to mitigate the COVID-19 pandemic effectively [5]. Kemp et al., 2021 [6] analyzed modified SEIR model and included the mutual interaction between vaccinations and social measures to explore the shape of the virus infection and hospitalizations. The model determines which vaccination rates are below to permit reaching herd immunity in 2021 by considering the social interaction parameter. [6]. Treesatayapun, 2022 [7] modified the SEIR model and considered the quarantined populations, effectively vaccinated, and ineffectively vaccinated individuals. The optimal vaccination strategy is estimated accompanied by the performance analysis [7]. De León et al., 2020 [8] proposed the SEIARD compartmental model to investigate the transmission dynamics of the coronavirus disease. Rafiq et al., 2022 [9] presented a new numerical scheme that generates a more realistic and accurate result of a complex bi-modal nonlinear model. Acheampong et al., 2022 [10] constructed a modified SEIR compartmental model to delineate the transmission dynamics of SARS-CoV-2 in Ghana and evaluate the basic reproduction number. Liu et al., 2021 [11] also proposed a Bayesian SEIR epidemiological model which can explain the transmission dynamics in the nine regions of England.

Gonzalez-Parra et al., 2021 [12] studied two different variants of the COVID-19 virus and presented a mathematical model for any other new variant. Kassa et al., 2020 [13] discussed the mitigation strategies for Covid-19 and performed sensitivity analysis. Sharov, 2020 [14] and Tong et al., 2021 [15] tried to demonstrate the efficacy of lockdown to control virus transmission and proposed the SIR model and its extension. Pai et al., 2020 [16] discussed the lockdown effect which is implemented in India to control the transmission of the coronavirus and evaluated the transmission dynamics of COVID-19. Huang et al., 2021 [17] presented an epidemiological model which demonstrated that combined effort of vaccination and maintaining physical distancing is a better strategy than stay-at-home. Şahin and Şahin, 2020 [18] compared three different models a) grey model (GM), b) nonlinear grey Bernoulli model (NGBM), and c) fractional nonlinear grey Bernoulli model (FANGBM) to identify properly a cumulative number of COVID-19 confirmed cases.

According to the high and low basic reproduction number, a multi-wave solution to the model of coronavirus was demonstrated by Shayak et al., 2021 [19]. A few numbers of researchers are considered the effect of vaccines in their proposed model to represent more specific transmission dynamics of the disease [3,12–15]. They performed SIR and SEIR mathematical models with a two-phase vaccination process. They assumed that those who received the first dose vaccine, may protect the disease certainly but there is a possibility to move in susceptible compartment whereas those who received second dose vaccines, may have almost zero possibility to be infected. Kuddus et al., 2021 [22] have investigated the effect of double dose vaccination rate, progression rate as well as transmission rate on the spread of measles. They observed that the transmission rate (β) from susceptible to exposed individuals had the most significant influence on measles prevalence.

Mathematically, the transmission of the disease will decrease when the effective reproduction number remain below 1. Moreover, a study to control the transmission dynamics of a virus is presented by Edward et al., 2015 [24] using the mathematical model. Sen et al., 2021 [25] proposed a new SEIR epidemic to explore the double-dose vaccination feedback. Gomes et al., 2022 [26] discussed the contribution of the vaccine to the acquisition of herd immunity in individuals. Annas et al., 2020 [27] designed their COVID-19 model to study the transmission dynamics of the virus by considering the vaccination and isolation factors. Moore et al., 2021 [28] employed a deterministic mathematical model to determine the efficiency of the vaccine to control long-term dynamics of coronavirus and their findings reveal that only double dose vaccination is insufficient to contain the outbreak. They stated that the vaccine will prevent 85% of infections which is estimated with the most optimistic assumption.

Deploy the optimal level of vaccination in the community is one of the best strategies to prevent the transmission of the disease which reduce the infection and death risk [29]. Yang et al., 2021 [30] studied the impact of mitigation, suppression, and multiple rolling interventions to prevent the transmission of COVID-19 in the UK and other European countries, accounting for the balance of healthcare demand. They proposed that rolling intervention is an optimal strategy that would reduce the overall infections and deaths due to the coronavirus as well as balance healthcare demand effectively in the UK [30]. Sah et al., 2021 [31] identified the impact of precipitated vaccine distribution which can reduce the burden due to the several variants of coronavirus. Martínez-Rodríguez et al., 2021 [32] also investigated the impact of the pace of vaccination and its efficacy on prevalence, hospitalizations, and deaths related to the coronavirus as well as identified different burden scenarios due to the SARS-CoV-2 virus. Fuady et al., 2021 [33] demonstrated several vaccines delivering strategies. To mitigate the negative impact of COVID-19, vaccination programs in the community should follow a proper distribution strategy [19].

Rahman and Kuddus, 2021 [34] demonstrated an age-structured Susceptible-Latent-Mild-Critical-Removed (SLMCR) compartmental model of COVID-19 disease transmission. Aguilar-Canto et al., 2022 [35] augmented a model of multiple vaccination strategies to control the disease. Ramos et al., 2021 [36] demonstrated a mathematical model to explore the impact of coronavirus variants as well as vaccines. Arruda et al., 2021 [37] presented a new epidemic model considering reinfection and multiple viral strains of the virus which are the latest challenge to prevent the current COVID- 19 situation. Leónet et al., 2022 [38] demonstrated the multiple strains of the SARS-CoV-2 and introduced a new epidemiological model that accounts for two different variants of the virus and the significance of the vaccination program.

In this study, we performed analytical and numerical simulations of COVID-19 model to depict the transmission dynamics of this disease. The next-generation matrix (NGM) technique is applied to estimate the basic reproduction number ($\Re_0$) for the disease dynamics of the system. We determined the existence and uniqueness of the system properties and solution for the disease-free (DFE) and disease endemic equilibrium (DEE). Sensitivity analysis of different parameters has been performed to recognize the most efficacious model parameters to spread the COVID-19 virus. The outcomes of this analysis provide direction to the policy-maker about the steps which are effective to mitigate the COVID-19 outbreak in Bangladesh. Finally, the numerical result represents that the transmission of the virus is significantly restricted if the susceptible individuals are fully vaccinated maintain all other health guidelines.

The remainder of this paper is organized as follows: in section 2 we presented mathematical formulation of COVID-19 model. The existence and uniqueness of the model, equilibrium points, and its stability and basic reproduction number are presented in section 3. In section 4, numerical simulation of the proposed model and sensitivity analysis are calculated with suitable parameters values. Finally, in section 5 a brief discussion of the model result is elucidated and a concluding remark is provided.

Mathematical model formulation and explanation

In this section, we developed a compartmental COVID-19 transmission dynamics model with the help of a system of ordinary differential equations among the following mutually exclusive compartments. Based on different considerations, a significant number of mathematical models for COVID-19 transmission dynamics have become omnipresent. A series of mathematical models have been analyzed to delineate the transmission dynamic pattern of infectious diseases [3,39–41]. We considered the total population size among nine mutually exclusive compartments: susceptible individuals, S(t), are uninfected people with the disease but a chance to be infected; the first dose vaccinated individuals, $V_1(t)$, though still have to chance to be infected; second doses vaccinated individuals, $V_2(t)$, those who have completed the both dose vaccination within on time; exposed individuals, E(t), are those who are

affected with a disease but have not yet developed respiratory illness; mild individuals, M(t), are indicated those who are asymptomatic; critical individuals, C(t), are express the COVID-19 symptoms clearly; non-hospitalized individuals, NH(t), are not in serious health crisis; hospitalized individuals, H(t), are those who are in critical health and respiratory crisis; and recovered individuals, R(t), are recovered against the disease who were infected. The recovery compartment contains those individuals who are already COVID-19 negative after treatment, home isolation, no longer contacting with others, or dead case. The proposed schematic diagram of our proposed COVID-19 model illustrates in Fig. 1.

The total size of the population, N(t) is assumed to be constant and well mixed:.

$$N(t) = S(t) + V_1(t) + V_2(t) + E(t) + M(t) + C(t) + NH(t) + H(t) + R(t) \quad (1)$$

In this model, all dead individuals are considered as newborns which are replaced in the susceptible compartment to keep the population size constant. A natural death case includes in all compartments at the constant per-capita rate μ and critical health-related deaths, which occur at the constant per-capita rate α. Peoples who received the first dose vaccine, shift to the vaccinated compartment (V_1) from the susceptible population (S) with the constant rate ϕ. Among the first dose vaccinated population, there is a rate (η) to move susceptible states, whereas the remaining populations progress out to the second dose of vaccinated population states (V_2) with a rate ρ. The full course vaccinated population moved to the recovery state (R) from the V_2 state at a constant rate ψ. In our model, we assumed that the net inflow of uninfected population to susceptible is at a rate of μN. Susceptible individuals are decreased with those people who become infected due to contact with the coronavirus at a rate β(M + C), where β represents the transmission rate of the virus. The infected individuals are then moved to the exposed state E. The exposed compartment contains those infected populations who are express mild or critical health crises. A number of populations of the exposed state transfer to the mild compartment (M) at a rate δ_1, whereas the remaining populations progress to the critical compartment at a per-capita rate δ_2. There are also some mild individuals who move to the critical compartment at a rate χ due to declining health immunity within a few days. Other mild individuals transfer to the non-hospital compartment at a rate γ. The population of the critical compartment (C) is transmitted to two compartments, named non-hospital and hospital, according to the health condition with a per-capita rate ω_1 and ω_2, respectively. The recovery rate of the population from the mild (M), non-hospital (NH), and hospital (H) compartments are κ, θ, and σ, respectively.

According to the proposed model, the transmission dynamics of the disease is designed with the following dynamic variables. A system of nonlinear ordinary differential equations delineates the model as.

$$\frac{dS}{dt} = \mu N - \beta S(M + C) - \phi S - \mu S + \eta V_1 \quad (2)$$

$$\frac{dV_1}{dt} = \phi S - \eta V_1 - \rho V_1 - \mu V_1 \quad (3)$$

$$\frac{dV_2}{dt} = \rho V_1 - \psi V_2 - \mu V_2 \quad (4)$$

$$\frac{dE}{dt} = \beta S(M + C) - \delta_1 E - \delta_2 E - \mu E \quad (5)$$

$$\frac{dM}{dt} = \delta_1 E - \chi M - \kappa M - \mu M - \gamma M \quad (6)$$

$$\frac{dC}{dt} = \delta_2 E + \chi M - \omega_1 C - \omega_2 C - \alpha C - \mu C \quad (7)$$

$$\frac{dNH}{dt} = \omega_1 C + \gamma M - \theta NH - \mu NH \quad (8)$$

$$\frac{dH}{dt} = \omega_2 C - \sigma H - \mu H \quad (9)$$

$$\frac{dR}{dt} = \kappa M + \theta NH + \sigma H + \psi V_2 - \mu R \quad (10)$$

with the positive initial conditions:.

$$S(0) = S_0 \geqslant 0, V_1(0) = V_{10} \geqslant 0, V_2(0) = V_{20} \geqslant 0, E(0) = E_0 \geqslant 0, M(0) = M_0 \geqslant 0, C(0) = C_0 \geqslant 0, NH(0) = NH_0 \geqslant 0, H(0) = H_0 \geqslant 0, R(0) = R_0 \geqslant 0 \quad (11)$$

The existence and positivity of the solution (for all $t \geq 0$) of the proposed model (2) - (10) with the initial conditions (11) can be easily performed.

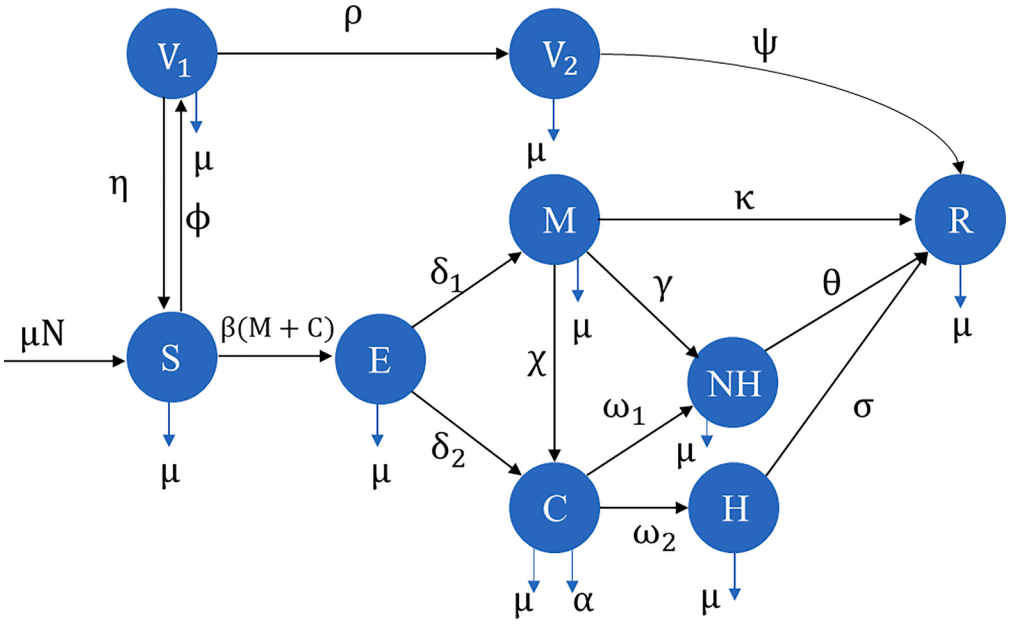

Fig. 1. Schematic flow diagram of the disease transmission model.

Quantitative analysis of the model

In this section, we have analyzed the invariant region, non-negativity of the solution, the existence of equilibria, disease-free and disease-endemic equilibrium points, basic reproduction number, stability analysis, and sensitivity analysis.

Positive invariance

We have analyzed the existence of the solution of the system (2) - (10) with the initial conditions (11) and investigated the nonnegativity condition of the dynamic variable for all $t \geq 0, \mathbb{R}^9_+$.

To demonstrate the nonnegativity, we assert the following theorem.

Theorem 3.1. Solutions of the all dynamic variable (S(t), V_1(t), V_2(t), E(t), M(t), C(t), NH(t), H(t), R(t)) of the system (2)-(10) with the initial conditions (11) satisfy $S(t) > 0$, $V_1(t) > 0$, $V_2(t) > 0$, $E(t) > 0$, $M(t) > 0$, $C(t) > 0$, $NH(t) > 0$, $H(t) > 0$, and $R(t) > 0$ for all $t > 0$, then the system (2)-(10) is positively invariant and attracting within $\mathbb{R}^9_+$.

Proof. We choose the Eq. (2) from the proposed model which can be written as.

$$\frac{dS}{dt} = \mu N - \beta S(M + C) - \phi S - \mu S + \eta V_1$$

$$\frac{dS}{dt} = \mu N + \eta V_1 - \tau S \tag{12}$$

where, $\tau = \beta(M + C) + \phi + \mu$

Integrating the above equation (12), we get the following expression.

$$S(t) = S_0 \exp\left(-\int_0^t \tau(u)du\right) + (\mu N + \eta V_1)\exp\left(-\int_0^t \tau(u)du\right) \int_0^t \left(\exp\int_0^s \tau(v)dv\right)ds \tag{13}$$

Hence the proof.

Positive invariance for all variables

In this section, we perform positive invariance for all other variables. From equation (3) of the model, we get.

$$\frac{dV_1}{dt} = \phi S - \eta V_1 - \rho V_1 - \mu V_1$$

$$\Rightarrow \frac{dV_1}{dt} \geq -(\eta + \rho + \mu)V_1 \tag{14}$$

Solving the above equation (14), we have the expression.

$$V_1(t) \geq V_{10}\exp\left(-\int_0^t (\eta + \rho + \mu)du\right) > 0 \tag{15}$$

which reveals that $V_1(t)$ is non-negative for all t, where V_{10} is the initial value (at $t = 0$). Similarly, we can deduce that solutions trajectories for the rest of the dynamic variables of the system remain positive for all $t > 0$ and they are:

$$V_2(t) \geq V_{20}\exp\left(-\int_0^t (\psi + \mu)du\right) > 0 \tag{16}$$

$$E(t) \geq E_0\exp\left(-\int_0^t (\delta_1 + \delta_2 + \mu)du\right) > 0 \tag{17}$$

$$M(t) \geq M_0\exp\left(-\int_0^t (\chi + \kappa + \gamma + \mu)du\right) > 0 \tag{18}$$

$$C(t) \geq C_0\exp\left(-\int_0^t (\omega_1 + \omega_2 + \alpha + \mu)du\right) > 0 \tag{19}$$

$$NH(t) \geq NH_0\exp\left(-\int_0^t (\theta + \mu)du\right) > 0 \tag{20}$$

$$H(t) \geq H_0\exp\left(-\int_0^t (\sigma + \mu)du\right) > 0 \tag{21}$$

$$R(t) \geq R_0\exp\left(-\int_0^t \mu du\right) > 0 \tag{22}$$

Boundedness

We analyzed the model (2) - (10) to determine the biological feasible solution set. The following theorem assure that the solutions of the system are bounded in the set with the non-negative conditions.

Theorem 3.2. The feasible solution set of the system– (2) - (10) subjected to the initial conditions (11) which initiate in $\mathbb{R}^9_+$ are uniformly bounded in ζ, where $\zeta = \{(S, V_1, V_2, E, M, C, NH, H, R) \in \mathbb{R}^9_+ : S + V_1 + V_2 + E + M + C + NH + H + R = N\}$is the positively invariant region.

Proof. Using the non-negative initial conditions (11) in the system– (2) - (10), it is observed that each of the dynamical variables remains non-negative (from Theorem 3.1). So, adding each of the equations (2) to (10), we obtain the total population size, N(t) which satisfies in the absence of death case owing to COVID-19 or if there is no critical individual (i.e., $C = 0$) [22], then we get.

$$\frac{dN}{dt} = \frac{dS}{dt} + \frac{dV_1}{dt} + \frac{dV_2}{dt} + \frac{dE}{dt} + \frac{dM}{dt} + \frac{dC}{dt} + \frac{dNH}{dt} + \frac{dH}{dt} + \frac{dR}{dt}$$

$$\Rightarrow \frac{dN}{dt} = \mu N - \mu S - \mu V_1 - \mu V_2 - \mu E - \mu M - \alpha C - \mu C - \mu NH - \mu H - \mu R$$

$$\Rightarrow \frac{dN}{dt} = 0,$$

Integrating the above equation, we have.

$$N(t) = \text{Constant}.$$

Accordingly, the constant size of the population, we obtain that all feasible solutions of each of the dynamical variables i.e., S, V_1, V_2, E, M, C, NH, H, and R are bounded in the invariant region.

Analysis of equilibria

In this analysis, we observed two equilibrium points in the system which are disease-free equilibrium (DFE) and disease-endemic equilibrium (DEE). When the basic reproduction number remains below one (i.e., $\Re_0 < 1$) we attain DFE, whereas if the basic reproduction number exceeds one (i.e., $\Re_0 > 1$), we attain DEE [22].

Disease-free equilibrium (DFE) point (X^0)

In this section, we determine the DFE point of the system (2)-(10) in which disease compartments are considered as zero. In this model, we considered nine compartments in which five are infected compartments, i.e., E, M, C, NH, H and another four compartments are uninfected states, i.e., S, V_1, V_2, and R. At the infection-free steady state $E = M = C = NH = H = R = 0$. Hence, the disease-free equilibrium point is:.

$$X^0 = (S^0, V_1^0, V_2^0, E^0, M^0, C^0, NH^0, H^0, R^0)$$

$$= \left(\frac{\mu N(\rho + \eta + \mu)}{(\mu + \rho)(\eta + \mu + \phi) - \eta\rho}, \frac{\phi\mu N}{(\mu + \rho)(\eta + \mu + \phi) - \eta\rho}, \frac{\phi\mu\rho N}{((\mu + \rho)(\eta + \mu + \phi) - \eta\rho)(\psi + \mu)}, 0, 0, 0, 0, 0, 0\right)$$

Disease-endemic equilibrium (DEE) point (X)*

Here, we determine the disease-endemic equilibrium point of the system (2)-(10) in which the disease spreads in the inhabitants. The endemic equilibrium point is discovered by equating zero of each of the equations of the system. Considering that every dynamic variable is non-zero i.e., $S^* \neq V_1^* \neq V_2^* \neq E^* \neq M^* \neq C^* \neq NH^* \neq H^* \neq R^* \neq 0$. Hence, the endemic equilibrium point is:.

$$X^* = \left(S^*, V_1^*, V_2^*, E^*, M^*, C^*, NH^*, H^*, R^*\right)$$

$$S^* = \frac{(\delta_1+\delta_2+\mu)(\chi+\kappa+\gamma+\mu)(\omega_1+\omega_2+\alpha+\mu)}{\beta((\omega_1+\omega_2+\alpha+\mu+\chi)\delta_1+(\chi+\kappa+\gamma+\mu)\delta_2)}$$

$$V_1^* = \frac{\phi(\delta_1+\delta_2+\mu)(\chi+\kappa+\gamma+\mu)(\omega_1+\omega_2+\alpha+\mu)}{\beta(\eta+\rho+\mu)((\omega_1+\omega_2+\alpha+\mu+\chi)\delta_1+(\chi+\kappa+\gamma+\mu)\delta_2)}$$

$$V_2^* = \frac{\rho\phi(\delta_1+\delta_2+\mu)(\chi+\kappa+\gamma+\mu)(\omega_1+\omega_2+\alpha+\mu)}{\beta(\psi+\mu)(\eta+\rho+\mu)((\omega_1+\omega_2+\alpha+\mu+\chi)\delta_1+(\chi+\kappa+\gamma+\mu)\delta_2)}$$

$$E^* = \frac{(\phi+\mu)(\Re_0-1)(\chi+\kappa+\gamma+\mu)(\omega_1+\omega_2+\alpha+\mu)}{\beta((\omega_1+\omega_2+\alpha+\mu+\chi)\delta_1+(\chi+\kappa+\gamma+\mu)\delta_2)}$$

$$M^* = \frac{(\phi+\mu)(\Re_0-1)(\omega_1+\omega_2+\alpha+\mu)\delta_1}{\beta((\omega_1+\omega_2+\alpha+\mu+\chi)\delta_1+(\chi+\kappa+\gamma+\mu)\delta_2)}$$

$$C^* = \frac{(\phi+\mu)(\Re_0-1)((\chi+\kappa+\gamma+\mu)\delta_2+\chi\delta_1)}{\beta((\omega_1+\omega_2+\alpha+\mu+\chi)\delta_1+(\chi+\kappa+\gamma+\mu)\delta_2)}$$

$$NH^* = \frac{(\phi+\mu)(\Re_0-1)((\chi+\kappa+\gamma+\mu)\delta_2\omega_1+(\omega_1+\omega_2+\alpha+\mu)\gamma\delta_1+\chi\delta_1\omega_1)}{\beta(\theta+\mu)((\omega_1+\omega_2+\alpha+\mu+\chi)\delta_1+(\chi+\kappa+\gamma+\mu)\delta_2)}$$

$$H^* = \frac{(\phi+\mu)(\Re_0-1)((\chi+\kappa+\gamma+\mu)\delta_2+\chi\delta_1)\omega_2}{\beta(\sigma+\mu)((\omega_1+\omega_2+\alpha+\mu+\chi)\delta_1+(\chi+\kappa+\gamma+\mu)\delta_2)}$$

$$R^* = \frac{\begin{array}{c}(\phi+\mu)(\Re_0-1)(\psi+\mu)\left(\begin{array}{c}((\chi+\kappa+\gamma+\mu)\delta_2+\chi\delta_1)((\sigma+\mu)\theta\omega_1+(\theta+\mu)\sigma\omega_2) \\ +(\omega_1+\omega_2+\alpha+\mu)((\theta+\mu)\kappa+\gamma\theta)(\sigma+\mu)\delta_1\end{array}\right) \\ +\frac{\psi\rho\phi(\delta_1+\delta_2+\mu)(\chi+\kappa+\gamma+\mu)(\omega_1+\omega_2+\alpha+\mu)(\sigma+\mu)(\theta+\mu)}{(\rho+\eta+\mu)}\end{array}}{\mu\beta(\sigma+\mu)(\theta+\mu)(\psi+\mu)((\omega_1+\omega_2+\alpha+\mu+\chi)\delta_1+(\chi+\kappa+\gamma+\mu)\delta_2)} \quad (23)$$

Eq. (23) reveals that if $\Re_0 > 1$ then the disease-endemic equilibrium point $X^* = (S^*, V_1^*, V_2^*, E^*, M^*, C^*, NH^*, H^*, R^*) \in \zeta$.

Basic reproduction number ($\Re_0$)

The basic reproduction number can be estimated as the spectral radius of a next generation matrix (NGM) using disease-free equilibrium point [42]. The NGM can be deduced by the product of two matrices T and $-\Sigma^{-1}$ where the matrix T represents the infection transmission rate in E, M, and C compartments and the matrix Σ delineate all other transitions across the compartments. The matrices T and Σ are expressed as:

$$T = \begin{bmatrix} 0 & \beta S^0 & \beta S^0 \\ 0 & 0 & 0 \\ 0 & 0 & 0 \end{bmatrix}, \text{ and}$$

$$\Sigma = \begin{bmatrix} -(\delta_1+\delta_2+\mu) & 0 & 0 \\ \delta_1 & -(\chi+\kappa+\gamma+\mu) & 0 \\ \delta_2 & \chi & (\omega_1+\omega_2+\alpha+\mu) \end{bmatrix}$$

The next generation matrix is

$$K = T \times (-\Sigma^{-1})$$

$$K = \begin{bmatrix} \frac{S^0\beta((\omega_1+\omega_2+\alpha+\mu+\chi)\delta_1+(\chi+\kappa+\gamma+\mu)\delta_2)}{(\delta_1+\delta_2+\mu)(\chi+\kappa+\gamma+\mu)(\omega_1+\omega_2+\alpha+\mu)} & \frac{S^0\beta(\omega_1+\omega_2+\alpha+\mu+\chi)}{(\chi+\kappa+\gamma+\mu)(\omega_1+\omega_2+\alpha+\mu)} & \frac{S^0\beta}{(\omega_1+\omega_2+\alpha+\mu)} \\ 0 & 0 & 0 \\ 0 & 0 & 0 \end{bmatrix}$$

The largest magnitude eigenvalue of the next generation matrix (K) denotes the basic reproduction number of the disease. So, by calculating the characteristic equation, $|K - \lambda I| = 0$, we can obtain the largest magnitude eigenvalue, where λ represents all possible eigenvalues and I represent the identity matrix. Hence, the basic reproduction number ($\Re_0$) is obtained as:

$$\Re_0 = \frac{S^0\beta((\omega_1+\omega_2+\alpha+\mu+\chi)\delta_1+(\chi+\kappa+\gamma+\mu)\delta_2)}{(\delta_1+\delta_2+\mu)(\chi+\kappa+\gamma+\mu)(\omega_1+\omega_2+\alpha+\mu)}$$

$$= \frac{\beta\mu N(\rho+\eta+\mu)((\omega_1+\omega_2+\alpha+\mu+\chi)\delta_1+(\chi+\kappa+\gamma+\mu)\delta_2)}{((\mu+\rho)(\eta+\mu+\phi)-\eta\rho)(\delta_1+\delta_2+\mu)(\chi+\kappa+\gamma+\mu)(\omega_1+\omega_2+\alpha+\mu)}$$

Stability analysis of the equilibrium point

In this section, we performed the stability analysis of the disease-free equilibrium (DFE) and disease-endemic equilibrium (DEE).

Theorem 3.3. *The disease-free equilibrium,* $X^0 = (S^0, V_1^0, V_2^0, 0, 0, 0, 0, 0, 0)$, *of the system* (2– 10) *is locally asymptotically stable if* $\Re_0 < 1$ *and unstable if* $\Re_0 > 1$.

Proof. To determine the stability of DFE i.e.,$X^0 = (S^0, V_1^0, V_2^0, 0, 0, 0, 0, 0, 0)$, we calculate the Jacobian matrix of the system (2) – (11), which is designate as:

$$J = \begin{bmatrix} -\beta(M+C)-\phi-\mu & \eta & 0 & 0 & -\beta S & -\beta S & 0 & 0 & 0 \\ \phi & -(\rho+\eta+\mu) & 0 & 0 & 0 & 0 & 0 & 0 & 0 \\ 0 & \rho & -(\psi+\mu) & 0 & 0 & 0 & 0 & 0 & 0 \\ -\beta(M+C) & 0 & 0 & -(\delta_1+\delta_2+\mu) & \beta S & \beta S & 0 & 0 & 0 \\ 0 & 0 & 0 & \delta_1 & -(\chi+\kappa+\gamma+\mu) & 0 & 0 & 0 & 0 \\ 0 & 0 & 0 & \delta_2 & \chi & -(\omega_1+\omega_2+\alpha+\mu) & 0 & 0 & 0 \\ 0 & 0 & 0 & 0 & \gamma & \omega_1 & -(\theta+\mu) & 0 & 0 \\ 0 & 0 & 0 & 0 & 0 & \omega_2 & 0 & -(\sigma+\mu) & 0 \\ 0 & 0 & \psi & 0 & \kappa & 0 & \theta & \sigma & -\mu \end{bmatrix}$$

At the infection-free equilibrium point(X^0), the Jacobian matrix is in form.

$$J(X^0) = \begin{bmatrix} -(\phi+\mu) & \eta & 0 & 0 & -\beta S^0 & -\beta S^0 & 0 & 0 & 0 \\ \phi & -(\rho+\eta+\mu) & 0 & 0 & 0 & 0 & 0 & 0 & 0 \\ 0 & \rho & -(\psi+\mu) & 0 & 0 & 0 & 0 & 0 & 0 \\ 0 & 0 & 0 & -(\delta_1+\delta_2+\mu) & \beta S^0 & \beta S^0 & 0 & 0 & 0 \\ 0 & 0 & 0 & \delta_1 & -(\chi+\kappa+\gamma+\mu) & 0 & 0 & 0 & 0 \\ 0 & 0 & 0 & \delta_2 & \chi & -(\omega_1+\omega_2+\alpha+\mu) & 0 & 0 & 0 \\ 0 & 0 & 0 & 0 & \gamma & \omega_1 & -(\theta+\mu) & 0 & 0 \\ 0 & 0 & 0 & 0 & 0 & \omega_2 & 0 & -(\sigma+\mu) & 0 \\ 0 & 0 & \psi & 0 & \kappa & 0 & \theta & \sigma & -\mu \end{bmatrix}$$

Now, we have to exhibit that all the eigenvalues of $J(X^0)$ are negative. The 9th column contains only the diagonal element $-\mu$ which indicates that $-\mu$ is one negative eigenvalue, whereas the remaining eigenvalues can be determined from the sub-matrix, $J_1(X^0)$. However, $J_1(X^0)$ matrix can be formed by eliminating the 9th row and 9th column of $J(X^0)$. Which gives,.

$$J_1(X^0) = \begin{bmatrix} -(\phi+\mu) & \eta & 0 & 0 & -\beta S^0 & -\beta S^0 & 0 & 0 \\ \phi & -(\rho+\eta+\mu) & 0 & 0 & 0 & 0 & 0 & 0 \\ 0 & \rho & -(\psi+\mu) & 0 & 0 & 0 & 0 & 0 \\ 0 & 0 & 0 & -(\delta_1+\delta_2+\mu) & \beta S^0 & \beta S^0 & 0 & 0 \\ 0 & 0 & 0 & \delta_1 & -(\chi+\kappa+\gamma+\mu) & 0 & 0 & 0 \\ 0 & 0 & 0 & \delta_2 & \chi & -(\omega_1+\omega_2+\alpha+\mu) & 0 & 0 \\ 0 & 0 & 0 & 0 & \gamma & \omega_1 & -(\theta+\mu) & 0 \\ 0 & 0 & 0 & 0 & 0 & \omega_2 & 0 & -(\sigma+\mu) \end{bmatrix}$$

In a similar way, the 3rd, 7th and 8th columns contain only the diagonal terms $-(\psi+\mu)$, $-(\theta+\mu)$, $-(\sigma+\mu)$, respectively, which form the negative eigenvalues. The rest of the eigenvalues can be evaluated from the reduced sub-matrix, $J_2(X^0)$ formed by eliminating the 3rd, 7th and 8th rows as well as corresponding columns from $J_1(X^0)$.

$$J_2(X^0) = \begin{bmatrix} -(\phi+\mu) & \eta & 0 & -\beta S^0 & -\beta S^0 \\ \phi & -(\rho+\eta+\mu) & 0 & 0 & 0 \\ 0 & 0 & -(\delta_1+\delta_2+\mu) & \beta S^0 & \beta S^0 \\ 0 & 0 & \delta_1 & -(\chi+\kappa+\gamma+\mu) & 0 \\ 0 & 0 & \delta_2 & \chi & -(\omega_1+\omega_2+\alpha+\mu) \end{bmatrix}$$

This matrix can be written in block form as:

$$J_2(X^0) = \begin{bmatrix} A_1 & A_2 \\ A_3 & A_4 \end{bmatrix}, \text{where} A_1 = \begin{bmatrix} -(\phi+\mu) & \eta \\ \phi & -(\rho+\eta+\mu) \end{bmatrix}, A_2 = \begin{bmatrix} 0 & -\beta S^0 & -\beta S^0 \\ 0 & 0 & 0 \end{bmatrix}$$

$$A_3 = \begin{bmatrix} 0 & 0 \\ 0 & 0 \\ 0 & 0 \end{bmatrix}, \text{and} A_4 = \begin{bmatrix} -(\delta_1+\delta_2+\mu) & \beta S^0 & \beta S^0 \\ \delta_1 & -(\chi+\kappa+\gamma+\mu) & 0 \\ \delta_2 & \chi & -(\omega_1+\omega_2+\alpha+\mu) \end{bmatrix}$$

$$\text{Since} A_3 = \begin{bmatrix} 0 & 0 \\ 0 & 0 \\ 0 & 0 \end{bmatrix}, \text{then we obtain,}$$

det (A_1 - λI)× det (A_4 - λI) = 0.

Now we can implement the Routh-Hurwitz stability criterion directly and independently to the matrices A_1 and A_4. We need to demonstrate that the trace of the both matrix is negative and the determinant is positive for the (2 × 2) A_1 matrix as well as negative for the (3 × 3) A_4 matrix. So, from the (2 × 2) A_1 matrix, we have

$$\text{trace}(A_1) = -(\phi+\mu) - (\rho+\eta+\mu) < 0,$$

stable if $\Re_0 < 1$. If either $\Re_0 > 1$, X^0 will be unstable i.e., the characteristic equation has at least one positive root with real part.

Theorem 3.4. The disease-endemic equilibrium point, X*, of the system (2)-(10) is locally asymptotically stable if $\Re_0 > 1$.

Proof: We obtain the Jacobian matrix of the system (2) – (10) at X*= (S*, V_1*, V_2*, E*, M*, C*, NH*, H*, R*) which can be expressed as:

$$J(X^*) = \begin{bmatrix} -\beta(M^*+C^*)-\phi-\mu & \eta & 0 & 0 & -\beta S^* & -\beta S^* & 0 & 0 & 0 \\ \phi & -(\rho+\eta+\mu) & 0 & 0 & 0 & 0 & 0 & 0 & 0 \\ 0 & \rho & -(\psi+\mu) & 0 & 0 & 0 & 0 & 0 & 0 \\ -\beta(M^*+C^*) & 0 & 0 & -(\delta_1+\delta_2+\mu) & \beta S^* & \beta S^* & 0 & 0 & 0 \\ 0 & 0 & 0 & \delta_1 & -(\chi+\kappa+\gamma+\mu) & 0 & 0 & 0 & 0 \\ 0 & 0 & 0 & \delta_2 & \chi & -(\omega_1+\omega_2+\alpha+\mu) & 0 & 0 & 0 \\ 0 & 0 & 0 & 0 & \gamma & \omega_1 & -(\theta+\mu) & 0 & 0 \\ 0 & 0 & 0 & 0 & 0 & \omega_2 & 0 & -(\sigma+\mu) & 0 \\ 0 & 0 & \psi & 0 & \kappa & 0 & \theta & \sigma & -\mu \end{bmatrix}$$

and $\det(A_1) = (\phi+\mu)(\rho+\eta+\mu) - \eta\phi = \phi(\rho+\mu) + \mu(\rho+\eta+\mu) > 0$

For (3x3) A_4 matrix, we get

Condition (1):

$$\text{trace}(A_4) = -(\delta_1+\delta_2+\mu) - (\chi+\kappa+\gamma+\mu) - (\omega_1+\omega_2+\alpha+\mu) < 0,$$

Condition (2):

The 9th column of $J(X^*)$ contains the diagonal element −μ which indicates that −μ is one negative eigenvalue, whereas the remaining eigenvalues can be determined from the sub-matrix, $J_1(X^*)$. $J_1(X^*)$ matrix can be formed by eliminating the 9th row and 9th column of J (X*). Which gives,

$$J_1(X^*) = \begin{bmatrix} -\beta(M^*+C^*)-\phi-\mu & \eta & 0 & 0 & -\beta S^* & -\beta S^* & 0 & 0 \\ \phi & -(\rho+\eta+\mu) & 0 & 0 & 0 & 0 & 0 & 0 \\ 0 & \rho & -(\psi+\mu) & 0 & 0 & 0 & 0 & 0 \\ \beta(M^*+C^*) & 0 & 0 & -(\delta_1+\delta_2+\mu) & \beta S^* & \beta S^* & 0 & 0 \\ 0 & 0 & 0 & \delta_1 & -(\chi+\kappa+\gamma+\mu) & 0 & 0 & 0 \\ 0 & 0 & 0 & \delta_2 & \chi & -(\omega_1+\omega_2+\alpha+\mu) & 0 & 0 \\ 0 & 0 & 0 & 0 & \gamma & \omega_1 & -(\theta+\mu) & 0 \\ 0 & 0 & 0 & 0 & 0 & \omega_2 & 0 & -(\sigma+\mu) \end{bmatrix}$$

Sum of minors of matrix A_4 along diagonal,

$$\begin{aligned} &= (\delta_1+\delta_2+\mu)(\chi+\kappa+\gamma+\mu) + (\delta_1+\delta_2+\mu)(\omega_1+\omega_2+\alpha+\mu) \\ &\quad + (\chi+\kappa+\gamma+\mu)(\omega_1+\omega_2+\alpha+\mu) \\ &\quad - \beta S^0(\delta_1+\delta_2) \end{aligned}$$

In a similar way, the 3rd, 7th and 8th columns contain only the diagonal terms −(ψ +μ), −(θ+μ), −(σ+μ), respectively, which form the negative eigenvalues. The rest of the eigenvalues can be evaluated from the reduced sub-matrix, $J_2(X^*)$ formed by eliminating the 3rd, 7th and

$$= (\delta_1+\delta_2+\mu)(\omega_1+\omega_2+\alpha+\mu)\left(1 - \frac{\Re_0(\chi+\kappa+\gamma+\mu)(\delta_1+\delta_2)}{((\omega_1+\omega_2+\alpha+\mu+\chi)\delta_1 + (\chi+\kappa+\gamma+\mu)\delta_2)}\right) + (\delta_1+\delta_2+\mu)(\chi+\kappa+\gamma+\mu) + (\chi+\kappa+\gamma+\mu)(\omega_1+\omega_2+\alpha+\mu) > 0,$$

for $\Re_0 < 1$.

Condition (3):

$$\begin{aligned} \det(A_4) &= S^0\beta((\omega_1+\omega_2+\alpha+\mu+\chi)\delta_1 + (\chi+\kappa+\gamma \\ &\quad +\mu)\delta_2) - (\delta_1+\delta_2+\mu)(\chi+\kappa+\gamma+\mu)(\omega_1+\omega_2+\alpha+\mu) \end{aligned}$$

$$= \frac{S^0\beta((\omega_1+\omega_2+\alpha+\mu+\chi)\delta_1 + (\chi+\kappa+\gamma+\mu)\delta_2)}{(\delta_1+\delta_2+\mu)(\chi+\kappa+\gamma+\mu)(\omega_1+\omega_2+\alpha+\mu)} - 1$$

$= \Re_0 - 1 < 0$ for any values of $\Re_0 < 1$.

Hence, the disease-free equilibrium X^0 is locally asymptotically

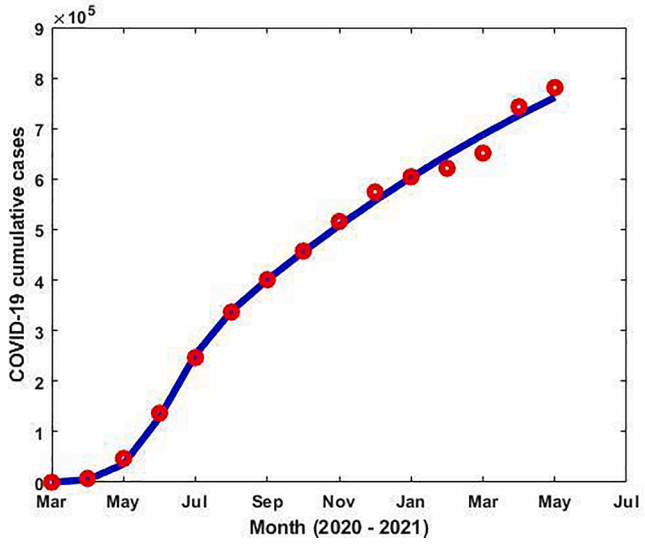

Fig. 2. Reported Bangladesh COVID-19 month-wise incidence data (red dot) and the corresponding best fit (blue solid curve). (For interpretation of the references to colour in this figure legend, the reader is referred to the web version of this article.)

Table 1
Description and estimated value of the model (2–10) parameters.

Parameters	Description	Estimated value	References
N	Total population	163,046,161	[45]
μ	Natural death rate	$\frac{1}{70}$ per year	[46]
η	Progression rate from V_1 to S	0.095	[3]
ϕ	First dose vaccination rate	0.64	Fitted
β	Transmission rate	1.0×10^{-6}	Fitted
ρ	Second dose vaccination rate	0.001	Fitted
ψ	Recovery rate due to the second dose of vaccine	0.8	[3]
δ_1	Progression rate from E to M	0.007	Fitted
δ_2	Progression rate from E to C	3.05×10^{-5}	Fitted
χ	Progression rate from M to C	0.3	[34]
α	Disease death rate only for critical compartment	0.125	[3]
γ	Progression rate from M to NH	0.99	Fitted
κ	Progression rate from M to R	0.02	[34]
ω_1	Progression rate from C to NH	0.13	[47]
ω_2	Progression rate from C to H	0.87	Fitted
θ	Recovery rate from NH to R	1/42	[30]
σ	Recovery rate from H to R	1/21	[30]

8th rows as well as corresponding columns from $J_1(X^*)$.

$$J_2(X^*) = \begin{bmatrix} -\beta(M^* + C^*) - (\phi + \mu) & \eta & 0 & -\beta S^* & -\beta S^* \\ \phi & -(\rho + \eta + \mu) & 0 & 0 & 0 \\ \beta(M^* + C^*) & 0 & -(\delta_1 + \delta_2 + \mu) & \beta S^* & \beta S^* \\ 0 & 0 & \delta_1 & -(\chi + \kappa + \gamma + \mu) & 0 \\ 0 & 0 & \delta_2 & \chi & -(\omega_1 + \omega_2 + \alpha + \mu) \end{bmatrix}$$

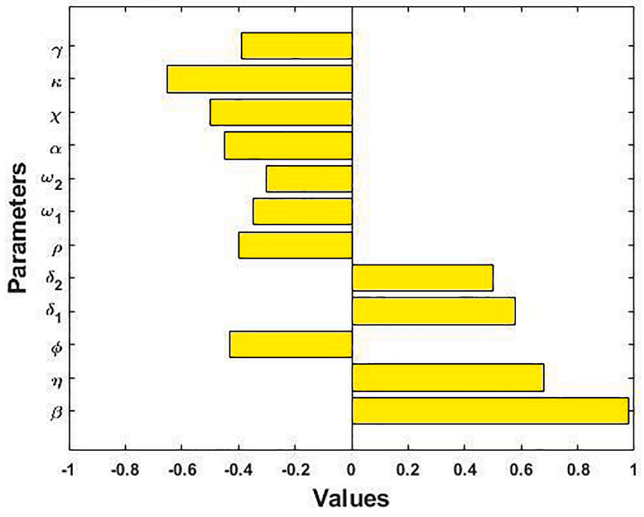

Fig. 3. Association between Mild cases (M^*) and the corresponding model parameters β, η, ϕ, δ_1, δ_2, ρ, ω_1, ω_2, α, χ, κ and γ.

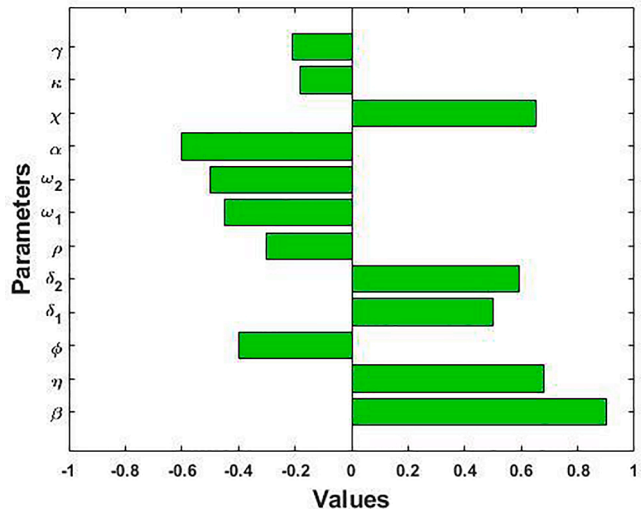

Fig. 4. Association between Critical cases (C^*) and the corresponding model parameters β, η, ϕ, δ_1, δ_2, ρ, ω_1, ω_2, α, χ, κ and γ.

Table 2
Sensitivity indices of $\Re_0$ for the parameters of our model (2–10).

Parameters	Description	Sensitivity index ($\Re_0$)
β	Transmission rate	+ 1.000
η	Progression rate from V_1 to S	+ 0.742
ϕ	First dose vaccination rate	− 0.861
δ_1	Progression rate from E to M	+ 0.667
δ_2	Progression rate from E to C	+ 0.0025
ρ	Second dose vaccination rate	− 0.048
ω_1	Progression rate from C to NH	− 0.024
ω_2	Progression rate from C to H	− 0.162
α	Disease death rate only for critical compartment	− 0.023
χ	Progression rate from M to C	− 0.018
κ	Progression rate from M to R	− 0.015
γ	Progression rate from M to NH	− 0.745

$$\Rightarrow J_2(X^*) = \begin{bmatrix} -\beta(M^*+C^*)-Q & \eta & 0 & -\beta S^* & -\beta S^* \\ \phi & -A & 0 & 0 & 0 \\ \beta(M^*+C^*) & 0 & -B & \beta S^* & \beta S^* \\ 0 & 0 & \delta_1 & -F & 0 \\ 0 & 0 & \delta_2 & \chi & -G \end{bmatrix} \text{where,}$$

$A = (\rho+\eta+\mu), B = (\delta_1+\delta_2+\mu), F = (\chi+\kappa+\gamma+\mu), G = (\omega_1+\omega_2+\alpha+\mu)$, and $Q = (\phi+\mu)$.

The characteristic equation of $J_2(X^*)$ is defined as,

$$|J_2(X^*) - \lambda I| = 0$$

$$\Rightarrow \begin{vmatrix} -\beta(M^*+C^*)-Q-\lambda & \eta & 0 & -\beta S^* & -\beta S^* \\ \phi & -A-\lambda & 0 & 0 & 0 \\ \beta(M^*+C^*) & 0 & -B-\lambda & \beta S^* & \beta S^* \\ 0 & 0 & \delta_1 & -F-\lambda & 0 \\ 0 & 0 & \delta_2 & \chi & -G-\lambda \end{vmatrix} = 0$$

$$\Rightarrow \lambda^5 + B_1\lambda^4 + B_2\lambda^3 + B_3\lambda^2 + B_4\lambda + B_5 = 0 \text{ (25) where,}$$

$$O = (\rho+\mu),\ B_1 = \beta(M^*+C^*) + A + B + F + G + Q$$

$$B_2 = ((M^*+C^*)(A+B+F+G) + S^*(\delta_1 + \delta_2))\beta + (F+G)(A+B) + (B+G+O)Q + (G+Q)F + AB + \eta\mu$$

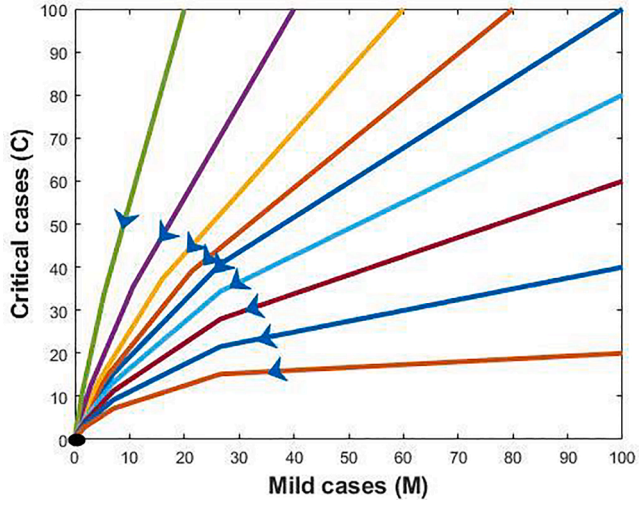

Fig. 5. Disease-free equilibrium: $\Re_0 < 1$. In this case, COVID-19 disease dies out (black dot).

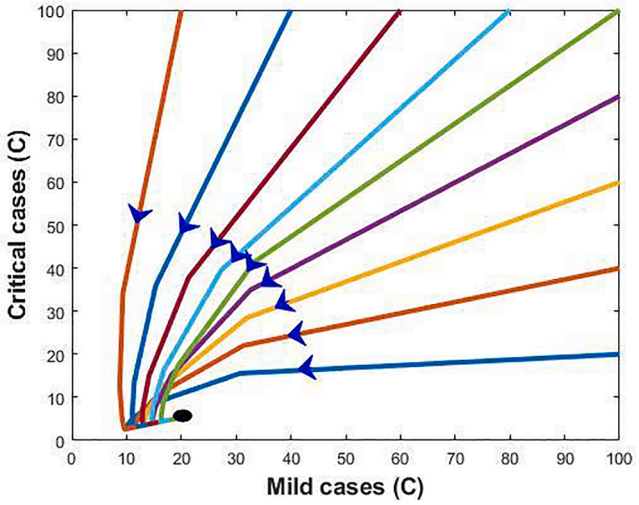

Fig. 6. Endemic equilibrium: $\Re_0 > 1$. In this case, COVID-19 disease persists in the community (black dot).

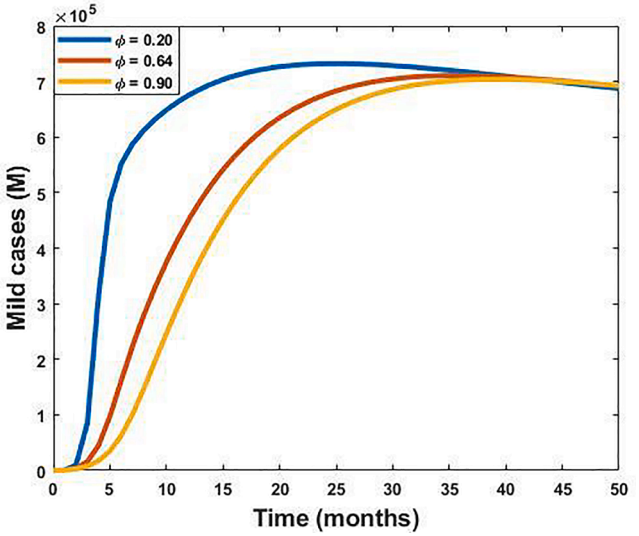

Fig. 7. Impact of first dose vaccine (ϕ) on the Mild cases (M).

$$B_3 = 2S^*(M^*+C^*)(\delta_1+\delta_2)\beta^2 + ((M^*+C^*)(A+B+G)+\delta_2 S^*)F\beta + (\delta_1(Q+\chi)+\delta_2 Q)\beta + (((M^*+C^*)(A+B)+\delta_1 S^*)G + ((M^*+C^*)B + (\delta_1+\delta_2)S^*)A)\beta + BFG + (A+Q)(BF+FG+BG) + (B+F+G)(OQ+\eta\mu)$$

$$B_4 = 2((\delta_1+\delta_2)A + \delta_2 F + \delta_1(G+\chi))(M^*+C^*)S^*\beta^2 + (A+Q)(\delta_2 F + \delta_1(G+\chi))S^*\beta + (M^*+C^*)(ABF+AFG+ABG+BFG)\beta + BFG(A+Q) + (\beta S^*\delta_1 + \beta S^*\delta_2 + BF + FG + BG)(OQ+\eta\mu)$$

$$B_5 = 2A(\delta_2 F + \delta_1(G+\chi))(M^*+C^*)S^*\beta^2 + ((\delta_2 F + \delta_1(G+\chi))\beta S^* + BFG)(OQ+\eta\mu) + ABFG\beta(M^*+C^*)$$

From equation (25), it is evident that $B_1 > 0$, $B_2 > 0$, $B_3 > 0$, $B_4 > 0$, $B_5 > 0$ if M* and C* > 0. From Eq. (24), it is shown that both M*and C* are positive if $\Re_0 > 1$. Hence, by Routh-Hurwitz stability criterion, the disease-endemic equilibrium points X* is locally asymptotically stable for $\Re_0 > 1$.

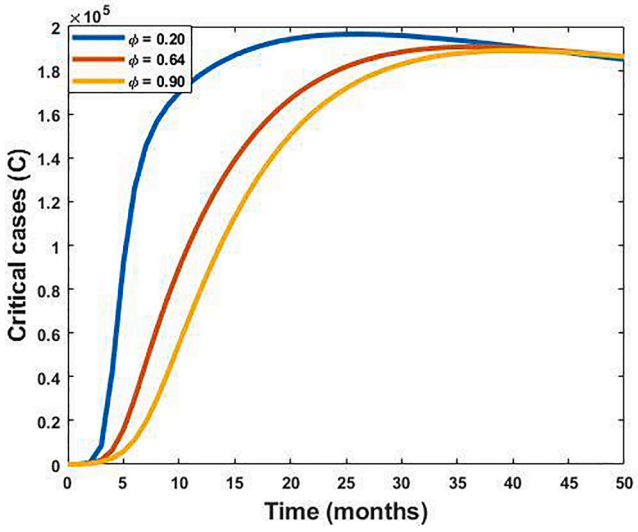

Fig. 8. Impact of first dose vaccine (ϕ) on the Critical cases (C).

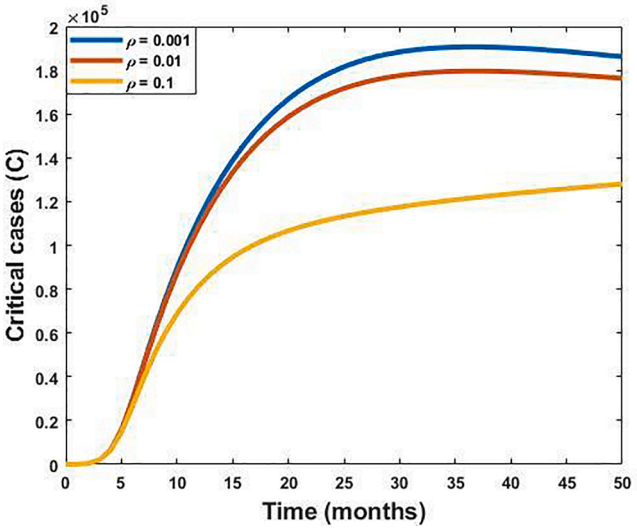

Fig. 10. Impact of second dose vaccine (ρ) on the Critical cases (C).

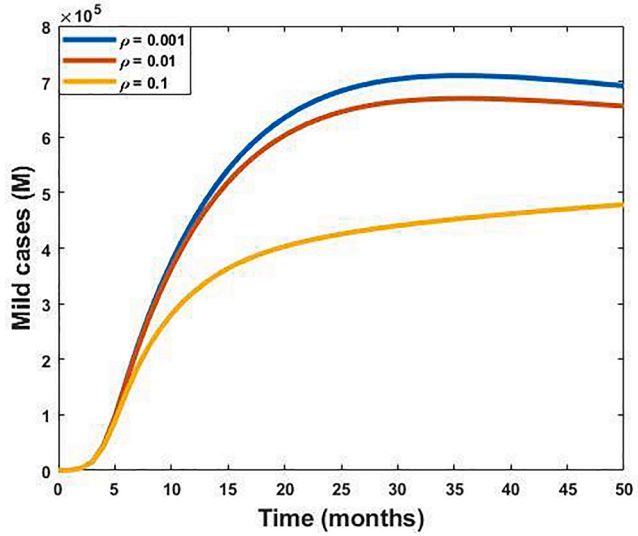

Fig. 9. Impact of second dose vaccine (ρ) on the Mild cases (M).

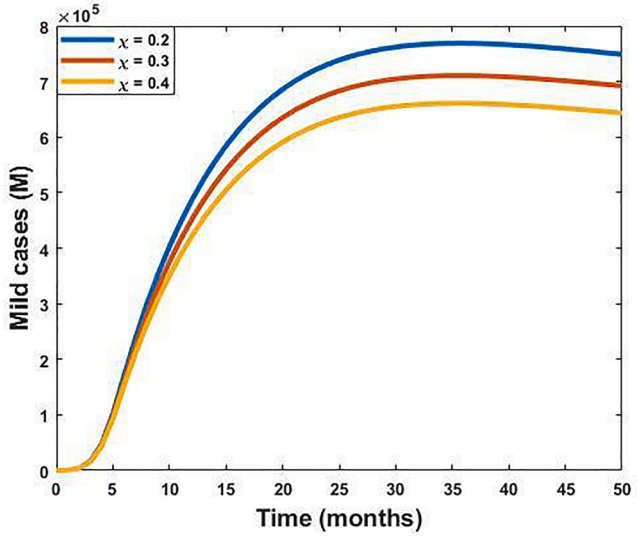

Fig. 11. Impact of co-infection (χ) on the Mild cases (M).

Numerical analysis of the model

Estimation of the parameter's value

First, COVID-19 infected individual was reported in Wuhan-China. The coronavirus transmits rapidly and spreads throughout China and after the whole world. The World Health Organization (WHO) has declared this situation as a global crisis, known as the Corona pandemic. In this section, we calibrated a month-wise reported number of COVID-19 cases in Bangladesh with our proposed model and estimate some specific parameters.

The value of the parameters in Eqs. (2)-(10), our considered COVID-19 model, is estimated by performing different combinations on the actual reported cases in Bangladesh from March 2020 to May 2021 [43]. Fig. 2 is shown the incidence data of COVID-19 from March 2020 to May 2021 (red dot) and the model fitted curve (blue solid curve) by employing the MATLAB routine. In particular, the proposed model is parameterized to handle the severe and mild health crisis due to COVID-19 in terms of the infected populations in Bangladesh. Here, we estimated some of the model parameter's value including transmission rate (β), first dose vaccination rate (ϕ), second dose vaccination rate (ρ), progression rate from E to M (δ_1), progression rate from E to C (δ_2), progression rate from M to NH (γ) and progression rate from C to H (ω_2), whereas rest of the parameter's value was taken from well-established literature (see Table 1). The estimation of the parameter's value is carried out with the help of the least-squares method which is implemented to minimize the summation of squared errors given by $\Sigma\,(Z(t, p) - N_{actual})^2$, with the proposed COVID-19 model (2)-(10), whereas N_{actual} is the actual number of COVID-19 confirmed cases and Z(t, p) demonstrate the solution of the model according to the number of infected individuals

during time t with the set of estimated parameters, p [44].

Evaluate the basic reproduction number ($\Re_0$)

The basic reproduction number of any disease illustrates how fast the disease becomes spread out into the susceptible populations. The disease can spread if the basic reproduction number, $\Re_0>1$. In this section, our goal is to estimate the numerical value of the basic reproduction number,$\Re_0$, of the model (2–10). Substituting the all-relative parameter's value in Eq. (24) from Table 1, we estimated the following result.

$$\Re_0 = \frac{\beta\mu N(\rho+\eta+\mu)((\omega_1+\omega_2+\alpha+\mu+\chi)\delta_1+(\chi+\kappa+\gamma+\mu)\delta_2)}{((\mu+\rho)(\eta+\mu+\phi)-\eta\rho)(\delta_1+\delta_2+\mu)(\chi+\kappa+\gamma+\mu)(\omega_1+\omega_2+\alpha+\mu)}$$

$$\Re_0 = \frac{1.0\times10^{-6}\times\frac{1}{70}\times163,046,161\times\left(0.001+0.095+\frac{1}{70}\right)\times\left(\left(0.13+0.87+0.125+\frac{1}{70}+0.3\right)\times0.007+\left(0.3+0.02+0.99+\frac{1}{70}\right)\times3.05\times10^{-5}\right)}{\left(\left(0.001+\frac{1}{70}\right)\left(0.095+0.64+\frac{1}{70}\right)-0.095\times0.001\right)\times\left(0.007+3.05\times10^{-5}+\frac{1}{70}\right)\times\left(0.3+0.02+0.99+\frac{1}{70}\right)\times\left(0.13+0.87+0.125+\frac{1}{70}\right)}\approx7.11$$

Hence, the value of the basic reproduction number ($\Re_0$) is approximately 7.11 which indicates that 7 or 8 susceptible populations can be infected by a single infected individual.

Sensitivity analysis

In this section, we implemented sensitivity analysis technique to determine the significance of each of the model parameters to control the SARS-CoV-2 virus transmission. Since this analysis is utilized to forecast model parameter's value about what should be done or avoided, so it has significant importance to preclude the transmission of the virus from human to human [48]. In this case, our intention is to evaluate the sensitivity index of the basic reproduction number ($\Re_0$) and the partial rank correlation coefficients (PRCC) for both Mild cases (M*) as well as Critical cases (C*) according to the model parameters. These two expressions are directly linked to reducing disease transmission [40]. That evaluation is performed with the help of Latin hypercube sampling, and the partial rank correlation coefficients (PRCC): a global sensitivity analysis method [22,49]. Here, we performed 100,000 simulations and a uniform distribution is allocated for each model parameter from 0 to 5 times their baseline value. The sign of the PRCCs indicates the increasing or decreasing effect on the outcome due to the corresponding increasing or decreasing value of each relative parameter. Identifying the significance of the parameters M*, and C*, by performing that method, we get an overall idea about which policies should be imposed to mitigate the spread of the disease. The PRCCs for the Mild cases, and Critical cases, shown in Figs. 3 and 4, have been determined by using the expressions M*, and C* from Eq. (23).

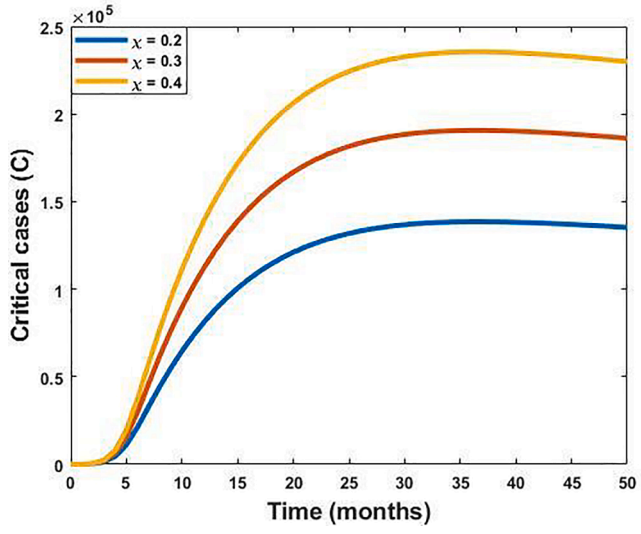

Fig. 12. Impact of co-infection (χ) on the Critical cases (C).

The association between Mild cases (M*) and Critical cases (C*) with the corresponding model parameters β, η, ϕ, δ_1, δ_2, ρ, ω_1, ω_2, α, χ, κ and γ are depicted in Fig. 3 and Fig. 4, respectively. Results represent that parameters β, η, δ_1, and δ_2 have a positive association with the model outcomes in both Mild cases (M*) and Critical case (C*) which indicates that the positive aspect of these parameters will accelerate up the value of M*, and C*. Moreover, the parameter χ has a positive aspect to soar the critical cases (C*). On the other hand, the parameters such as ϕ, ρ, ω_1, ω_2, α, κ, and γ have a negative association with the model outcomes, which reveals that increasing these parameters will decrease Mild and Critical cases.

The normalized forward sensitivity index of basic reproduction number ($\Re_0$) with respect to each of the parameter x_i can be derived as:

$$\Upsilon_{\Re_0}^{x_i} = \frac{\partial\Re_0}{\partial x_i}\times\frac{x_i}{\Re_0} \tag{26}$$

Using the above expression (26) and the value of the parameter from Table 1, we evaluate the sensitivity indices of the parameters for $\Re_0$ (see Table 2). From these indices, it is shown that the following parameters (β, η, ϕ, δ_1, δ_2, ρ, ω_1, ω_2, α, χ, κ, and γ) have significant importance to control the reproduction number.

Table 2 reveals the sensitivity indices of the basic reproduction number ($\Re_0$) with respect to the corresponding parameters. In the sensitivity indices, the most sensitive parameter to spread the disease in the community is the transmission rate (β). Other sensitive parameters are η, δ_1, and δ_2. That is, β, η, δ_1, δ_2 have a great impact to transmit the disease if their corresponding values get increased. Hence, increasing (or decreasing) the transmission rate (β) of the virus by 100%, the basic reproduction number ($\Re_0$) also increases (or decreases) by 100%.

On the other hand, the second most significant parameter to prevent the disease is the first dose vaccination rate (ϕ). Also, the parameter (γ) as the progression rate from a mild case to a non-hospital case has great significance to keep under control the disease. Other parameters such as ρ, ω_1, ω_2, α, χ, κ have negative sensitivity indices. The least sensitive parameter is the progression rate from a mild case to the recovery stage (κ).

Numerical simulations

In this section, we performed numerical simulations of our proposed model using the Ordinary Differential Equation (ODE) solvers in Matlab programming language to support the analytical results. For illustration we have selected baseline parameter values (see Table 1) consistent with COVID-19 infection and transmission. In accordance with the analytical results we found two equilibrium points: the disease-free equilibrium (X^0) and a disease-endemic equilibrium (X^*). From the numerical perspectives, the local stability of the disease-free equilibrium and disease-endemic equilibrium are investigated through standard dynamical systems analysis methods. Numerical results of the transmission dynamics for the equilibrium points of the disease are depicted in Figs. 5 and 6. In Fig. 5, we used different initial conditions of all state variables to depict the system of trajectories in the disease-free and disease-endemic equilibrium. We found that if the basic reproduction number ($\Re_0 < 1$) remains below one, the disease-free equilibrium is locally asymptotically stable which means that the disease will be fade-out from the community. However, Fig. 6 illustrates the stability of the disease-endemic equilibrium ($\Re_0 > 1$) by depicting system trajectories through the M VS C plane originating from different initial conditions. In this system the virus persists in the community.

Figs. 7 and 8 illustrate the effect of the first dose vaccine (ϕ) on the mild cases (M) and critical cases (C). From these figures, we observed that the infection case in both mild and critical cases can be reduced significantly if we increase the first dose vaccination rate sufficiently. The first dose vaccine (ϕ) rate has a negative correlation to control the outspread (from Table 2). From the public health perspective, the first dose vaccine prepares the immune system to fight against COVID-19 infection in the non-infected human body. The first dose vaccination reduces the chance to be infected though there is the possibility to be infected by the rate (η). The number of critical cases decreases if we increase first dose vaccination rate as shown in Fig. 8.

Figs. 9 and 10 depict the effect of the second dose vaccine (ρ) on the mild cases (M) and critical cases (C), respectively. Analyzing the figures, we can conclude that both doses of vaccine have more significance to reduce the risk of an outbreak. When the rate of the second dose of vaccination (ρ) escalated from 0.001 to 0.1; we observe that both mild and critical cases decrease effectively. Moreover, when $\rho = 0.1$ the number of mild and critical cases quickly decreases as shown in Figs. 9 and 10. We recommended that the second dose vaccine is essential to get maximum protection from COVID-19 which triggers continuously the immune system to produce a large number of antibodies.

Patients infected by COVID-19 may also have co-infection and can move from Mild case (M) Critical case (C). Among the mild individuals who face a sudden serious illness admitted to the hospital and consider that people as critical individuals. The co-infection rate (χ) has a negative correlation with the mild cases (M), whereas it has a positive correlation with the critical cases (C). From Fig. 11, we observed that mild case reduces due to the co-infection with other diseases and move to the critical compartment. Since the co-infection (χ) rate has a positive effect on the critical case. Therefore, the critical cases increase due to the increase of the co-infection which is shown in Fig. 12.

Discussion and conclusion

The new-confirmed cases of COVID-19 are increasing throughout the world and the transmission of coronavirus disease in human-to-human is the most concerning issue. In this situation, protecting public health with proper vaccination and imposing optimal strategies with limited resources is the highest priority to prevent the disease. Here, we proposed a modified SEIR compartmental disease model and examined it mathematically to investigate the transmission dynamics of COVID-19 based on accessible data.

In this study, we performed analytical and numerical simulations of the model and found two equilibrium points: the disease-free equilibrium point and a disease-endemic equilibrium point. We also estimated the basic reproduction number ($\Re_0$) and showed that both the equilibrium points of the system are locally asymptotically stable. From that analysis, we can conclude that the disease will approximately fade-out from the community when the basic reproduction number is less than one whereas, the disease persists in the community if the basic reproduction number is greater than one.

The proposed mathematical model has considered double doses vaccination program since Bangladesh started to provide vaccines to people on February 7, 2021. The first dose vaccination (ϕ) rate takes the first step to prevent the outbreak of the disease. Those persons who take the first dose vaccine, are not facing critical medical conditions. Medical experts have recommended getting both doses of the COVID vaccine to prevent infection. The second dose vaccine has a significant impact on antibody growth which is very essential to protect the COVID-19. The second dose vaccine stimulates the memory cells so that the body remembers this injection for the long term. It continuously triggers the immune system of the body to produce a large number of antibodies, resulting in cell-mediated immunity.

From the expression of basic reproduction number$\Re_0$, we found that it has positive correlation with the transmission rate (β), progression rate to be again infected (η), progression rate from exposed to mild as well as critical cases (δ_1 and δ_2, respectively). To explore the effect of the model parameters in disease transmission, sensitivity analysis has been performed which shows that the transmission rate (β) is 100% responsible for spreading the disease, presented in Table 2. Therefore, to control the disease we impose a strategy to minimize the transmission rate of the virus. The most effective strategy is ensuring vaccination which has up to 86.1% possibility to preclude the transmission of the virus (see Table 2). This study draws special attention to controlling the transmission of the virus in the community with the significance of first and second-dose vaccination on mild cases and critical cases. To prevent the disease transmission from the community, we must have to concern about the health cautions such as ware a face mask, maintain a safe distance and frequently wash the hands. Further, we numerically explored the impact of first and second doses vaccination rates on the dynamics of the COVID-19 outbreak. The numerical simulation has demonstrated that both dose vaccination has a negative impact on mild and critical cases. Therefore, an optimal vaccination program for all people, as well as home isolation for infected people, may protect most of the population from the outbreak of the virus in Bangladesh.

Funding source

This work was not funded and did not receive any specific grant from funding agencies in the public, commercial, or not-for-profit sectors.

CRediT authorship contribution statement

Anip Kumar Paul: Data curation, Writing – original draft, Methodology, Visualization, Validation, Software, Formal analysis. **Md Abdul Kuddus:** Conceptualization, Software, Writing – review & editing, Investigation, Visualization, Formal analysis, Validation, Supervision.

Declaration of Competing Interest

The authors declare that they have no known competing financial interests or personal relationships that could have appeared to influence the work reported in this paper.

References

[1] Korber B, Fischer WM, Gnanakaran S, Yoon H, Theiler J, Abfalterer W, et al. Tracking changes in SARS-CoV-2 spike: evidence that D614G increases infectivity of the COVID-19 virus. Cell 2020;182(4):812–827.e19.
[2] World Health Organization (WHO). Access to https://covid19.who.int/.

[3] Tilahun GT, Demie S, Eyob A. Stochastic model of measles transmission dynamics with double dose vaccination. Infect Dis Model 2020;5:478–94.
[4] Muller K, Muller PA. Mathematical modelling of the spread of COVID-19 on a university campus. Infect Dis Model 2021;6:1025–45.
[5] Musa SS, Qureshi S, Zhao S, Yusuf A, Mustapha UT, He D. Mathematical modeling of COVID-19 epidemic with effect of awareness programs. Infect Dis Model 2021;6:448–60.
[6] Kemp F, Proverbio D, Aalto A, Mombaerts L, Fouquier d'Hérouël A, Husch A, et al. Modelling COVID-19 dynamics and potential for herd immunity by vaccination in Austria, Luxembourg and Sweden. J Theor Biol 2021;530:110874. https://doi.org/10.1016/j.jtbi.2021.110874.
[7] Treesatayapun C. Epidemic model dynamics and fuzzy neural-network optimal control with impulsive traveling and migrating: Case study of COVID-19 vaccination. Biomed Signal Process Control 2022;71:103227. https://doi.org/10.1016/j.bspc.2021.103227.
[8] Avila-Ponce de León U, Pérez ÁGC, Avila-Vales E. An SEIARD epidemic model for COVID-19 in Mexico: Mathematical analysis and state-level forecast. Chaos, Solitons Fractals 2020;140:110165. https://doi.org/10.1016/j.chaos.2020.110165.
[9] Rafiq M, Ali J, Riaz MB, Awrejcewicz J. Numerical analysis of a bi-modal COVID-19 sitr model. Alex Eng J 2022;61(1):227–35.
[10] Acheampong E, Okyere E, Iddi S, Bonney JHK, Asamoah JKK, Wattis JAD, et al. Mathematical modelling of earlier stages of COVID-19 transmission dynamics in Ghana. Results Phys 2022;34:105193. https://doi.org/10.1016/j.rinp.2022.105193.
[11] Liu Y, Tang JW, Lam TTY. Transmission dynamics of the COVID-19 epidemic in England. Int J Infect Dis 2021;104:132–8.
[12] Gonzalez-Parra G, Martínez-Rodríguez D, Villanueva-Micó RJ. Impact of a new SARS-CoV-2 variant on the population: A mathematical modeling approach. Math Comput Appl 2021;26(2):25.
[13] Kassa SM, Njagarah JBH, Terefe YA. Analysis of the mitigation strategies for COVID-19: from mathematical modelling perspective. Chaos Solitons Fractals 2020;138:109968. https://doi.org/10.1016/j.chaos.2020.109968.
[14] Sharov KS. Creating and applying SIR modified compartmental model for calculation of COVID-19 lockdown efficiency. Chaos Solitons Fractals 2020;141:110295. https://doi.org/10.1016/j.chaos.2020.110295.
[15] Tong Z-W, Lv Y-P, Din RU, Mahariq I, Rahmat G. Global transmission dynamic of SIR model in the time of SARS-CoV-2. Results Phys 2021;25:104253. https://doi.org/10.1016/j.rinp.2021.104253.
[16] Pai C, Bhaskar A, Rawoot V. Investigating the dynamics of COVID-19 pandemic in India under lockdown. Chaos Solitons Fractals 2020;138:109988. https://doi.org/10.1016/j.chaos.2020.109988.
[17] Huang Bo, Wang J, Cai J, Yao S, Chan PKS, Tam T-W, et al. Integrated vaccination and physical distancing interventions to prevent future COVID-19 waves in Chinese cities. Nat Hum Behav 2021;5(6):695–705.
[18] Şahin U, Şahin T. Forecasting the cumulative number of confirmed cases of COVID-19 in Italy, UK and USA using fractional nonlinear grey Bernoulli model. Chaos Solitons Fractals 2020;138:109948. https://doi.org/10.1016/j.chaos.2020.109948.
[19] Shayak B, Sharma MM, Gaur M, Mishra AK. Impact of reproduction number on the multiwave spreading dynamics of COVID-19 with temporary immunity: A mathematical model. Int J Infect Dis 2021;104:649–54.
[22] Kuddus MA, Mohiuddin M, Rahman A. Mathematical analysis of a measles transmission dynamics model in Bangladesh with double dose vaccination. Sci Rep 2021;11(1):1–16.
[24] Edward S, Raymond KE, Gabriel KT, Nestory F, Godfrey MG, Arbogast MP. A mathematical model for control and elimination of the transmission dynamics of measles. Appl Comput Math 2015;4(6):396–408.
[25] Sen MDL, Alonso-Quesada S, Ibeas A, Nistal R. On a discrete seir epidemic model with two-doses delayed feedback vaccination control on the susceptible. Vaccines 2021;9(4):398.
[26] M. Gomes MG, Ferreira MU, Corder RM, King JG, Souto-Maior C, Penha-Gonçalves C, et al. Individual variation in susceptibility or exposure to SARS-CoV-2 lowers the herd immunity threshold. J Theor Biol 2022:111063. https://doi.org/10.1016/j.jtbi.2022.111063.
[27] Annas S, Isbar Pratama M, Rifandi M, Sanusi W, Side S. Stability analysis and numerical simulation of SEIR model for pandemic COVID-19 spread in Indonesia. Chaos Solitons Fractals 2020;139:110072. https://doi.org/10.1016/j.chaos.2020.110072.
[28] Moore S, Hill EM, Tildesley MJ, Dyson L, Keeling MJ. Vaccination and non-pharmaceutical interventions for COVID-19: a mathematical modelling study. Lancet Infect Dis 2021;21(6):793–802.
[29] Coccia M. Optimal levels of vaccination to reduce COVID-19 infected individuals and deaths: A global analysis. Environ Res 2022;204:112314. https://doi.org/10.1016/j.envres.2021.112314.
[30] Yang Po, Yang G, Qi J, Sheng B, Yang Y, Zhang S, et al. The effect of multiple interventions to balance healthcare demand for controlling COVID-19 outbreaks: a modelling study. Sci Rep 2021;11(1). https://doi.org/10.1038/s41598-021-82170-y.
[31] Sah P, Vilches TN, Moghadas SM, Fitzpatrick MC, Singer BH, Hotez PJ, et al. Accelerated vaccine rollout is imperative to mitigate highly transmissible COVID-19 variants. EClinicalMedicine 2021;35:100865. https://doi.org/10.1016/j.eclinm.2021.100865.
[32] Martínez-Rodríguez D, Gonzalez-Parra G, Villanueva RJ. Analysis of key factors of a SARS-CoV-2 vaccination program: A mathematical modeling approach. Epidemiologia 2021;2(2):140–61.
[33] Fuady A, Nuraini N, Sukandar KK, Lestari BW. Targeted vaccine allocation could increase the covid-19 vaccine benefits amidst its lack of availability: A mathematical modeling study in indonesia. Vaccines 2021;9(5):462.
[34] Rahman A, Kuddus MA. Modelling the Transmission Dynamics of COVID-19 in Six High-Burden Countries. Biomed Res Int 2021;2021:1–17. https://doi.org/10.1155/2021/5089184.
[35] Aguilar-Canto FJ, de León U-P, Avila-Vales E. Sensitivity theorems of a model of multiple imperfect vaccines for COVID-19. Chaos Solitons Fractals 2022;156:111844. https://doi.org/10.1016/j.chaos.2022.111844.
[36] Ramos AM, Vela-Pérez M, Ferrández MR, Kubik AB, Ivorra B. Modeling the impact of SARS-CoV-2 variants and vaccines on the spread of COVID-19. Commun Nonlinear Sci Numer Simul 2021;102:105937. https://doi.org/10.1016/j.cnsns.2021.105937.
[37] Arruda EF, Das SS, Dias CM, Pastore DH, Khudyakov YE. Modelling and optimal control of multi strain epidemics, with application to COVID-19. PLoS ONE 2021;16(9):e0257512.
[38] de León U-P, Avila-Vales E, Huang K-L. Modeling COVID-19 dynamic using a two-strain model with vaccination. Chaos Solitons Fractals 2022;157:111927. https://doi.org/10.1016/j.chaos.2022.111927.
[39] Kuddus MA, Rahman A. Analysis of COVID-19 using a modified SLIR model with nonlinear incidence. Results Phys 2021;27:104478. https://doi.org/10.1016/j.rinp.2021.104478.
[40] Asamoah JKK, Jin Z, Sun G-Q, Seidu B, Yankson E, Abidemi A, et al. Sensitivity assessment and optimal economic evaluation of a new COVID-19 compartmental epidemic model with control interventions. Chaos Solitons Fractals 2021;146:110885. https://doi.org/10.1016/j.chaos.2021.110885.
[41] Samui P, Mondal J, Khajanchi S. A mathematical model for COVID-19 transmission dynamics with a case study of India. Chaos Solitons Fractals 2020;140:110173. https://doi.org/10.1016/j.chaos.2020.110173.
[42] Diekmann O, Heesterbeek JAP, Roberts MG. The construction of next-generation matrices for compartmental epidemic models. J R Soc Interface 2010;7(47):873–85.
[43] WHO. Measles: Number of Reported Cases in Bangladesh (WHO, 2020).
[44] Olaniyi S, Obabiyi OS, Okosun KO, Oladipo AT, Adewale SO. Mathematical modelling and optimal cost-effective control of COVID-19 transmission dynamics. Eur Phys J 2020;135(11):1–20.
[45] Economy, C. Bangladesh Population in 2019. https://countryeconomy.com/demography/population/bangladesh (2020).
[46] Yang Y, Li J, Ma Z, Liu L. Global stability of two models with incomplete treatment for tuberculosis. Chaos Solitons Fractals 2010;43(1-12):79–85.
[47] WHO. Report of the WHO-China joint mission on coronavirus disease 2019 (COVID-19). Geneva, 2020.
[48] Islam MS, Ira JI, Kabir KA, Kamrujjaman M. COVID-19 Epidemic compartments model and Bangladesh. 2020. DOI: 10.20944/preprints202004.0193.v1.
[49] Asamoah JKK, Jin Z, Sun GQ, Li MY. A deterministic model for Q fever transmission dynamics within dairy cattle herds: using sensitivity analysis and optimal controls. Comput Math Methods Med 2020;3:1–18. https://doi.org/10.1155/2020/6820608.

Further reading

[20] Foy BH, Wahl B, Mehta K, Shet A, Menon GI, Britto C. Comparing COVID-19 vaccine allocation strategies in India: A mathematical modelling study. Int J Infect Dis. 2021;103:431–8. https://doi.org/10.1016/j.ijid.2020.12.075.
[21] Rocha Filho TM, Moret MA, Chow CC, Phillips JC, Cordeiro AJA, Scorza FA, et al. A data-driven model for COVID-19 pandemic–Evolution of the attack rate and prognosis for Brazil. Chaos Solitons Fractals. 2021;152:111359. https://doi.org/10.1016/j.chaos.2021.111359.
[23] Ochoche JM, Gweryina RI. A mathematical model of measles with vaccination and two phases of infectiousness. IOSR-JM. 2014;10(1):95–105. https://doi.org/10.9790/5728-101495105.